Tumor Suppressor Function of the Plasma Glutathione Peroxidase Gpx3 in Colitis-Associated Carcinoma

Caitlyn W. Barrett[1,2], Wei Ning[1,2], Xi Chen[4], Jesse Joshua Smith[5], Mary K. Washington[3], Kristina E. Hill[1], Lori A. Coburn[1,7], Richard M. Peek[1,2,6], Rupesh Chaturvedi[1,3], Keith T. Wilson[1,2,3,6,7], Raymond F. Burk[1], and Christopher S. Williams[1,2,6,7]

Abstract

The glutathione peroxidases, a family of selenocysteine-containing redox enzymes, play pivotal roles in balancing the signaling, immunomodulatory, and deleterious effects of reactive oxygen species (ROS). The glutathione peroxidase GPX3 is the only extracellular member of this family, suggesting it may defend cells against ROS in the extracellular environment. Notably, GPX3 hypermethylation and underexpression occur commonly in prostate, gastric, cervical, thyroid, and colon cancers. We took a reverse genetics approach to investigate whether GPX3 would augment inflammatory colonic tumorigenesis, a process characterized by oxidative stress and inflammation, comparing *Gpx3*$^{-/-}$ mice in an established two-stage model of inflammatory colon carcinogenesis. *Gpx3*-deficient mice exhibited an increased tumor number, though not size, along with a higher degree of dysplasia. In addition, they exhibited increased inflammation with redistribution toward protumorigenic M2 macrophage subsets, increased proliferation, hyperactive WNT signaling, and increased DNA damage. To determine the impact of acute gene loss in an established colon cancer line, we silenced *GPX3* in human Caco2 cells, resulting in increased ROS production, DNA damage and apoptosis in response to oxidative stress, combined with decreased contact-independent growth. Taken together, our results suggested an immunomodulatory role for GPX3 that limits the development of colitis-associated carcinoma. *Cancer Res; 73(3); 1245–55. ©2012 AACR.*

Introduction

Inflammatory bowel disease (IBD), which affects 1 in 600 Americans, is characterized by severe and chronic inflammation. Such inflammation is a known contributor to cancer as it promotes an environment rich in chemokines, cytokines, and reactive oxygen species (ROS) influencing epithelial proliferation and survival programs and impacting genomic integrity (1, 2). For example, patients with IBD show increased nitric oxide production via activated macrophages and granulocytes and increased plasma levels of the marker for DNA damage 8-hydroxydeoxyguanosine (1, 3). As such, the risk for cancer is increased 6-fold in patients with IBD compared with the general population, and cancer, or risk thereof, is a cause of significant morbidity in IBD (4).

Selenium is a necessary trace element that is present in the primary structure of selenoproteins as selenocysteine. Several epidemiologic studies have inversely correlated nutritional selenium status with colon and prostate cancer risk, although this is somewhat controversial. The effect of selenium status in IBD has not been definitively evaluated. It is proposed that the effect of selenium on carcinogenesis is realized by the selenoproteins into which it is incorporated. In support of this, mouse models with impaired selenoprotein expression show increased aberrant crypt foci, a preneoplastic colon lesion, and breast cancer incidence (5, 6). The selenocysteine present in the catalytic triad of glutathione peroxidases is optimized by hydrogen bonding with glutamine and tryptophan residues, enhancing its activity and, in the case of certain glutathione peroxidases, such as GPX1, this allows it to exert antioxidant activity (7, 8). One mechanism, though by no means the only, by which glutathione peroxidases may reduce cancer risk is by blunting the tumor-promoting effects of oxidative stress.

Gpx3, or plasma glutathione peroxidase, is the only known selenocysteine-containing extracellular form of glutathione peroxidase (Gpx) and accounts for nearly all of the glutathione peroxidase activity in plasma (9). *Gpx3* mRNA is expressed in a tissue-specific manner by the kidney, heart, lung, liver, brain, adipose tissue, breast, and gastrointestinal tract, but the majority of plasma Gpx3 is kidney-derived (10–12). It is likely that other organs contribute to plasma Gpx3 as nephrectomized rats retain 30% of original glutathione peroxidase

Authors' Affiliations: [1]Department of Medicine, Division of Gastroenterology; Departments of [2]Cancer Biology, [3]Pathology, Microbiology, and Immunology, and [4]Division of Cancer Biostatistics, Department of Biostatistics; [5]Section of Surgical Sciences, Department of Surgery, Division of Surgical Oncology, Vanderbilt University School of Medicine; [6]Vanderbilt Ingram Cancer Center; and [7]Veterans Affairs Tennessee Valley Health Care System, Nashville, Tennessee

Note: Supplementary data for this article are available at Cancer Research Online (http://cancerres.aacrjournals.org/).

C.W. Barrett and W. Ning contributed equally to this work.

Corresponding Author: Christopher S. Williams, Vanderbilt University School of Medicine, B2215 Garland Ave., 1065D MRB-IV, Nashville, TN 37232. Phone: 615-322-3642; Fax: 615-343-6229; E-mail: christopher.williams@vanderbilt.edu

doi: 10.1158/0008-5472.CAN-12-3150

©2012 American Association for Cancer Research.

Downloaded from http://aacrjournals.org/cancerres/article-pdf/73/3/1245/2692160/1245.pdf by guest on 24 May 2025

activity (13). Gpx3 is transported via circulation where it binds to the basement membranes of epithelial cells such as those in the gastrointestinal tract (14). *Gpx3* promoter hypermethylation and downregulation is commonly seen in human cancer (15–18). In prostate cancer, hemizygous and homozygous deletions as well as methylation of the first exon of *Gpx3* frequently occur (17). Promoter hypermethylation insures decreased expression of Gpx3 in gastric, cervical, thyroid, head and neck, and lung cancers, and in melanoma (15, 16) suggesting that Gpx3 serves as a tumor suppressor in these cancers. Genetic evidence supports a role for GPX enzymes in IBD with Gpx1;Gpx2 double knockout mice developing spontaneous ileocolitis (19) and intestinal carcinoma that is associated with bacteria-induced inflammation (20). In fact, Gpx2 alone may have a protective role in inflammatory carcinogenesis (21). The role of Gpx3 in these processes has never been directly tested.

We hypothesized that loss of Gpx3 would enhance tumorigenesis in inflammatory carcinogenesis, a process rich in ROS production and chemokine/cytokine–driven proproliferative stromal signals (1, 2, 22–24). To test this, we applied the azoxymethane/dextran sodium sulfate (AOM/DSS) murine inflammatory carcinogenesis model to $Gpx3^{-/-}$ mice. This model has been used to identify modifiers of colitis-associated carcinoma including NF-κB (25), TLR4 (26), TNF-α (27), and Mtgr1 (28), as well as innate immune responses (29) and intestinal microflora (30). We found a striking increase in tumor number in the absence of Gpx3, indicating a direct impact of Gpx3 on tumor initiation. In support of an initiating role, $Gpx3^{-/-}$ mice showed increased DNA damage. Tumors in $Gpx3^{-/-}$ mice showed increased inflammation as well as increased infiltration of M2 macrophages, proliferation, and nuclear β-catenin. $Gpx3^{-/-}$ tumors were also more advanced. As expected, knockdown of Gpx3 in the human colon cancer cell line Caco2 resulted in increased ROS production and DNA damage. Thus, we provide genetic evidence that Gpx3 behaves as a potent tumor suppressor during inflammatory carcinogenesis *in vivo* likely by decreasing the ROS and DNA damage that lead to tumor initiation.

Materials and Methods

Murine inflammatory carcinogenesis and chronic colitis protocols

Seven- to 8-week-old C57Bl/6 wild-type (WT; $n = 17$) or congenic $Gpx3^{-/-}$ ($n = 20$) mice were injected with 12.5 mg/kg of AOM (Sigma-Aldrich) intraperitoneally as described in Greten and colleagues (25). After a 3-day recovery period, the animals were started on the first of 4 cycles of 3% DSS *ad libitum* (see schematic in Fig. 1A). Each cycle lasted 5 days and was separated by a 16-day recovery period. A second DSS-only control arm was included for C57Bl/6 WT ($n = 14$) and $Gpx3^{-/-}$ ($n = 19$) that followed the same protocol outlined earlier excluding the AOM injection. After the last cycle, animals were sacrificed following a 26-day recovery period. Tumor counts and measurements were conducted in a blinded fashion under a stereo dissecting microscope. Each colon was then bisected longitudinally and half was Swiss-rolled for microscopic analysis and the other half was partitioned into normal and tumor tissue and saved for protein and RNA analysis. Microscopic analysis was conducted by a gastrointestinal pathologist (M.K. Washington) for severity of inflammation (31) and dysplasia on hematoxylin and eosin (H&E)–stained "Swiss rolled" colons (processed by the Vanderbilt Translational Pathology Shared Resource core). Four days after the third cycle of DSS, murine endoscopy was used to monitor colitis severity (32) and tumor burden. All *in vivo* procedures

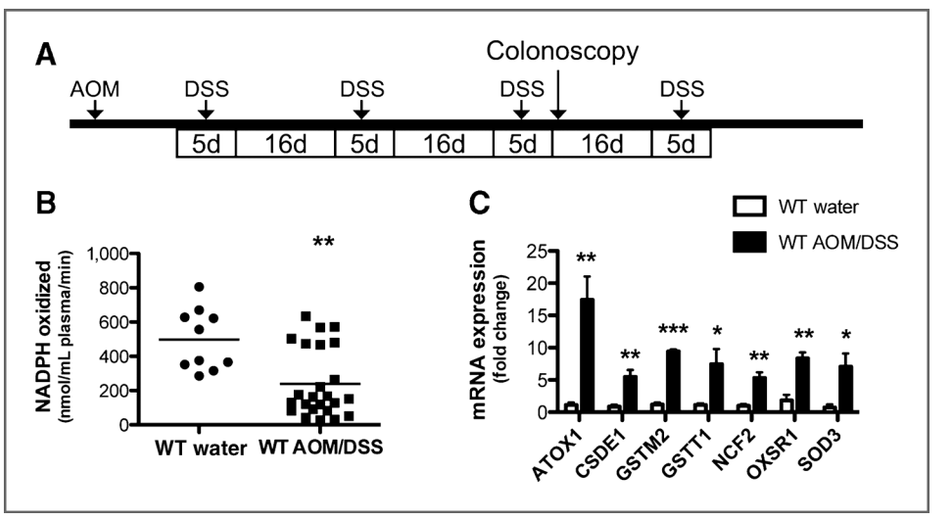

Figure 1. Plasma Gpx3 activity is decreased and oxidative stress genes are increased in mice subjected to the AOM/DSS protocol. A, schematic of the AOM/DSS protocol. Animals injected with 12.5 mg/kg AOM at day 0 followed by 4 cycles of 3% DSS *ad libitum* separated by 16 days of recovery on water. B, plasma glutathione peroxidase activity determined after the completion of the AOM/DSS protocol. WT water treated, $N = 10$; WT AOM/DSS, $N = 11$; **, $P = 0.0013$. C, tumor tissue mRNA expression of oxidative stress genes (ATOX1, ATX1 antioxidant protein 1 homolog; CSDE1, cold shock domain containing E1, RNA binding; GSTM2, glutathione S-transferase M2, muscle; GSTT1, glutathione S-transferase theta 1; NCF2, neutrophil cytosolic factor 2; OXSR1, oxidative-stress responsive 1; SOD3, superoxide dismutase 3, extracellular) in WT water treated ($N = 4$) vs. WT AOM/DSS ($N = 4$); ***, $P < 0.001$; **, $P < 0.01$; *, $P < 0.05$.

Downloaded from http://aacrjournals.org/cancerres/article-pdf/73/3/1245/2692160/1245.pdf by guest on 24 May 2025

were carried out in accordance with protocols approved by the Vanderbilt Institutional Animal Care and Use Committee.

Plasma glutathione peroxidase activity assay

Blood was collected from mice via the vena cava and plasma was separated from erythrocytes (K_3EDTA) by centrifugation at 12,000 rpm for 1 minute. Glutathione peroxidase activity was determined according to a modified protocol (33) based on the method of Paglia and Valentine (34). Briefly, 800 μL reaction cocktail [50 mmol/L potassium phosphate, pH 7.0, 1 mmol/L EDTA, 1 mmol/L NaN_3, 0.2 mmol/L NADPH, 1 EU/mL oxidized glutathione (GSSG)-reductase, and 1 mmol/L glutathione (GSH)] was mixed with 20 μL plasma and 80 μL water in a clear plastic cuvette and incubated at room temperature for 5 minutes. Hundred microliter hydrogen peroxide (H_2O_2) substrate (0.25 mmol/L H_2O_2 in H_2O) was added to the reaction mixture to initiate reaction. Gpx activity was assessed by measuring the rate of change of A_{340} per minute over a 3-minute time period after the addition of H_2O_2 to the reaction mixture. The enzymatic reaction is linear during this time period. The rate of change was then converted to the number of μmol NADPH oxidized per minute using the extinction coefficient of 6.2×10^3 L mol^{-1} cm^{-1} for NADPH at 340 nm. Blank reactions with plasma replaced by distilled water were subtracted from each assay.

Oxidative stress gene RT-PCR

RNA was made from 30 mg WT water treated colons and normal adjacent tissue from AOM/DSS colons using the RNeasy Mini kit (Qiagen), according to the manufacturer's directions. cDNA was then made using the SuperScript cDNA kit (Invitrogen). Real-time PCR (RT-PCR) was then conducted using an oxidative stress primer library (HOSL-1, Realtimeprimers.com). Reactions were conducted according to the manufacturer's recommendations. Analysis was conducted using the $\Delta\Delta C_t$ method.

Immunohistochemistry and immunofluorescence

Five-micrometer sections were cut, dewaxed, hydrated, and endogenous peroxidase activity quenched with 0.03% H_2O_2 in MeOH. Antigen retrieval was conducted using the boiling sodium citrate method in a microwave (20 mmol sodium citrate pH 6.5) for 16 minutes at 30% power. After blocking, primary antibody was added [α-Ki67 (NeoMarkers), 1:1,000; α-8-hydroxy-2′ deoxyguanosine (Abcam) 1:50; α-β-catenin (BD Transduction Laboratories), 1:1,000; α-arginase I (Arg1; Santa Cruz), 1:500; α-interleukin (IL)-1β (R&D Systems), 1:50; fluorescein isothiocyanate (FITC)-α-F4/80 (eBioscience), 1:1,000] and incubated overnight at 4°C. Isotype-matched antibodies were included as negative controls. The Vectastain ABC Elite System (Vector Laboratories) was used to visualize staining for immunohistochemistry. Identification of intratumoral apoptotic cells was conducted using the ApopTag Plus Peroxidase *In Situ* Apoptosis Kit (Chemicon) according to the manufacturer's protocol. Control H_2O_2 was obtained by omitting the terminal transferase (TnT) enzyme. For immunofluorescence staining of macrophage markers and DNA damage, slides were counterstained and mounted with ProLong Gold antifade including 4′,6-diamidino-2-phenylindole (DAPI; Invitrogen). Gpx3 staining was conducted as described (14). Immune cell, apoptosis, and proliferation indices were generated by counting the number of positive cells per high-powered field (HPF; ×40 objective) within each tumor by a blinded observer. A β-catenin index was used, as previously reported (28). This index is generated by multiplying the staining intensity (on a scale of 1–4) by percentage of the cells showing nuclear staining. The average score was then calculated for each Swiss-rolled colon.

Cell culture and short hairpin RNA knockdown

Caco2 human colon tumor cells were obtained from American Type Culture Collection (HTB-37) and had morphologic characteristics consistent with their known identity. Formal authentication was not conducted. Caco2 cells were maintained in Dulbecco's Modified Eagle's Medium (DMEM) supplemented with 10% FBS and penicillin/streptomycin. HEK293T cells were maintained in RPMI-1640 supplemented with 10% FBS and penicillin/streptomycin. HEK293T packaging cells were transfected with Mission short hairpin RNA (shRNA) constructs (Sigma-Aldrich) specific for human Gpx3 (clone ID: TRCN0000273651-NM, TRCN0000273684, and TRCN0000008678) as well as the PAX2 and pMD2.G plasmids using the calcium phosphate transfection method. Twenty-four hours posttransfection, medium was removed from the HEK293T cells and passed through a 0.45 μmol/L filter. A total of 4 μg/mL polybrene (Millipore) was added to the filtered media. Growth medium was removed from Caco2 cells and replaced with infection medium. After 6 hours, the infection medium was replaced with normal growth medium and the infection process was repeated 24 hours later. Cells were selected for knockdown using 5 μg/mL puromycin (Invitrogen) over a 3-day period. Knockdown was analyzed by the $\Delta\Delta C_t$ method following RT-PCR using Gpx3-specific TaqMan probes (Invitrogen) and by Western blotting using rabbit anti-mouse Gpx3 8096 (dilution 1:5,000; custom-made by Rockland).

ROS determination

Caco2 cells infected with either scrambled or Gpx3-specific shRNA were pretreated with 500 U/mL PEGylated catalase (PEG-CAT, Sigma) 1 hour before 1.5-hour treatment with 200 μmol/L H_2O_2. Either ROS detection reagent 6-carboxy-2′,7′-dichlorodihydrofluorescein diacetate, di(acetoxymethyl ester; DCFH2; Invitrogen) or the oxidation insensitive analog of DCFH2 (DCF; Invitrogen) was used to stain treated cells according to the manufacturer's protocol for flow cytometry analysis. In short, cells plated on a 6-well plate in phenol red–free medium were washed with 500 μL PBS. Cells were then resuspended in 1 μmol/L DCFH2 or 0.5 μmol/L DCF in prewarmed PBS and incubated for either 20 or 5 minutes at 37°C, respectively. Cells were then washed twice with PBS and centrifuged at 1,600 rpm for 6 minutes between washes. Cells were analyzed for positivity by flow cytometry.

Detection of DNA damage and active caspase-3 by flow cytometry

Caco2 (sh-scrambled) and Caco2 (sh-hGpx3) cells were treated with H_2O_2 (100 μmol/L) for 4 hours and washed with

Downloaded from http://aacrjournals.org/cancerres/article-pdf/73/3/1245/2692160/1245.pdf by guest on 24 May 2025

PBS, fixed in 0.1% paraformaldehyde, and permeabilized with 100% methanol on ice. Levels of DNA damage and active caspase-3 were assessed as described previously (35). In brief, cells were incubated with rabbit antiactive caspase-3 antibody conjugated with phycoerythrin (PE; dilution 1:50; BD Biosciences) and 8-oxoguanosine–binding peptide conjugated with FITC (dilution 1:100) for 30 minutes at room temperature. Cells were acquired with a BD LSRII system (BD Biosciences) and analyzed using FlowJo software (Star tree).

Matrigel colony formation assay

The day before Matrigel plating, Matrigel (BD, 354234) at 9 mg/mL was thawed overnight in ice at 4°C. For each well of a 48-well plate, 50 μL ice-cold Caco2 media (DMEM supplemented with 10% FBS and penicillin/streptomycin) was mixed with 50 μL Matrigel. Plates were then allowed to solidify at 37°C for 30 minutes. Caco2 cells were trypsinized, washed with PBS, and diluted to 10,000 cells/mL in 2 mL media. A 1:1 mixture of cells and Matrigel was added to the wells in the prepared 48-well plate and incubated at 37°C for 30 minutes. To avoid drying, 200 μL complete Caco2 media was added to each Matrigel-filled well. Cells were maintained at their normal growth conditions and media was changed every 2 to 3 days. On day 22, cells were counted using GelCount (Oxford Optronix).

Results

Glutathione peroxidase activity is decreased and oxidative stress is increased in AOM/DSS-treated mice

Gpx3 is often downregulated in cancer (15–18) and we sought to determine whether its expression or activity was altered in the AOM/DSS model of inflammatory carcinogenesis. For these experiments, 7- to 8-week-old mice were injected with AOM and treated with 4 cycles of DSS as defined in Materials and Methods and shown in Fig. 1A. During the course of this protocol, 6 $Gpx3^{-/-}$ mice died (lost over 20% of original body weight and were sacrificed), 2 after cycle 1, 2 after cycle 2, and 2 during cycle 4 of DSS. Although, as is typical with this protocol, 2 WT mice died, both after cycle 4, a time when we usually see mortality. These mice were not included in the final analysis. This increased morbidity suggests that Gpx3 may protect the mucosa from DSS induced injury.

As decreased Gpx3 levels are commonly seen in cancer, we first tested plasma Gpx3 activity in mice receiving water only versus mice after the AOM/DSS protocol to determine if Gpx3 activity might be altered. Measurement of oxidation of NADPH allowed us to determine that AOM/DSS leads to diminished plasma glutathione peroxidase activity (497.7 ± 56.9 vs. 239.4 ± 40.8 nmol NADPH oxidized/mL plasma/min; $P = 0.0013$; Fig. 1B). As this indicated that there was a systemic decrease in glutathione peroxidase activity and protein levels of Gpx3 in the plasma validated glutathione peroxidase activity assays (Supplementary Fig. S1), we next wanted to determine if local Gpx3 mRNA levels were affected in AOM/DSS tumorigenesis. There was no difference in *Gpx3* mRNA expression between matched tumor and adjacent normal mucosa samples (Supplementary Fig. S2), but other oxidative stress response genes were upregulated in normal adjacent colon tissue from AOM/DSS mice (Fig. 1C) suggesting an increase in oxidant stress resulting from the protocol. Finally, we wanted to determine if *GPX3* expression varied in a large colorectal cancer expression array dataset, and in this case *GPX3* was markedly and consistently underexpressed as early as the adenoma stage (Supplementary Fig. S3A). We confirmed this observation with 10 matched normal/colon cancer samples by RT-PCR, and in a second set of 10 matched samples by protein analysis, finding reduced *GPX3* levels in 80% of the samples (Supplementary Fig. S3B and S3C). These results support previous studies (18) and suggest that GPX3 may serve as a tumor suppressor in colorectal cancer.

Gpx3 is a tumor suppressor in inflammatory tumorigenesis

Using the $Gpx3^{-/-}$ mouse, we directly tested whether Gpx3 was a tumor suppressor in the AOM/DSS model. Seven- to 8-week-old WT or $Gpx3^{-/-}$ mice were placed on the AOM/DSS protocol (Fig. 1A). As expected, mice lost weight and had looser stools as the result of DSS administration in both the DSS and AOM/DSS arms of the experiment (Supplementary Fig. S4), though there was no significant difference between genotypes in these parameters. Gpx3 protein is normally seen in the colon binding the basement membrane on the basolateral surface (ref. 14; Fig. 2A). $Gpx3^{-/-}$ mice showed an increased endoscopic colitis score (36) during both DSS and AOM/DSS protocols (Fig. 2B) with colonic thickening, vascular changes, evidence of fibrin, increased granularity, and softer stools than wild-type mice (DSS: 12.1 ± 1.4, $N = 6$ vs. 6.8 ± 1.0, $N = 6$; AOM/DSS: 12.1 ± 1.2, $N = 4$ vs. 6.9 ± 0.8; $N = 6$; $P < 0.01$ for both comparisons). Twenty-six days after the last DSS cycle the animals were sacrificed. Consistent with a role for Gpx3 in tumor suppression, quantification of tumor number in AOM/DSS mice showed increased tumor multiplicity in $Gpx3^{-/-}$ mice (21.1 ± 1.6 tumors/mouse $N = 11$ vs. 10.8 ± 1.5 tumors/mouse $N = 12$; $P < 0.0001$). In addition, there was a trend toward increased tumor number and size in $Gpx3^{-/-}$ mice receiving DSS only without AOM when compared with wild-type mice (1.0 ± 0.3 tumors/mouse $N = 18$ vs. 0.4 ± 0.2 tumors/mouse, $N = 13$; $P = 0.1$, Fig. 2C).

Histologic examination by a gastrointestinal pathologist (M.K. Washington) of H&E-stained sections from colons prepared as "Swiss Rolls" revealed increased injury severity based on a multiparameter histologic injury score (31) in $Gpx3^{-/-}$ AOM/DSS mice (16.2 ± 2.6 $N = 14$ vs. 7.8 ± 0.92 $N = 16$; $P = 0.003$, Fig. 3A and B) with significant increases in inflammation, inflammation extent, and crypt damage/regeneration (Fig. 3C). Tumors were also analyzed for grade and $Gpx3^{-/-}$ adenomas showed increased propensity for high-grade dysplasia characterized by loss of polarity and a more complex tumor growth pattern than WT tumors (Fig. 3D). In fact, one $Gpx3^{-/-}$ tumor showed local invasion (Fig. 3A and D), a property rarely seen in response to AOM/DSS. These results suggest that Gpx3 loss results in increased colonic injury and inflammation and contributes to tumor promotion and progression in the AOM/DSS model of inflammatory carcinogenesis.

Downloaded from http://aacrjournals.org/cancerres/article-pdf/73/3/1245/2692160/1245.pdf by guest on 24 May 2025

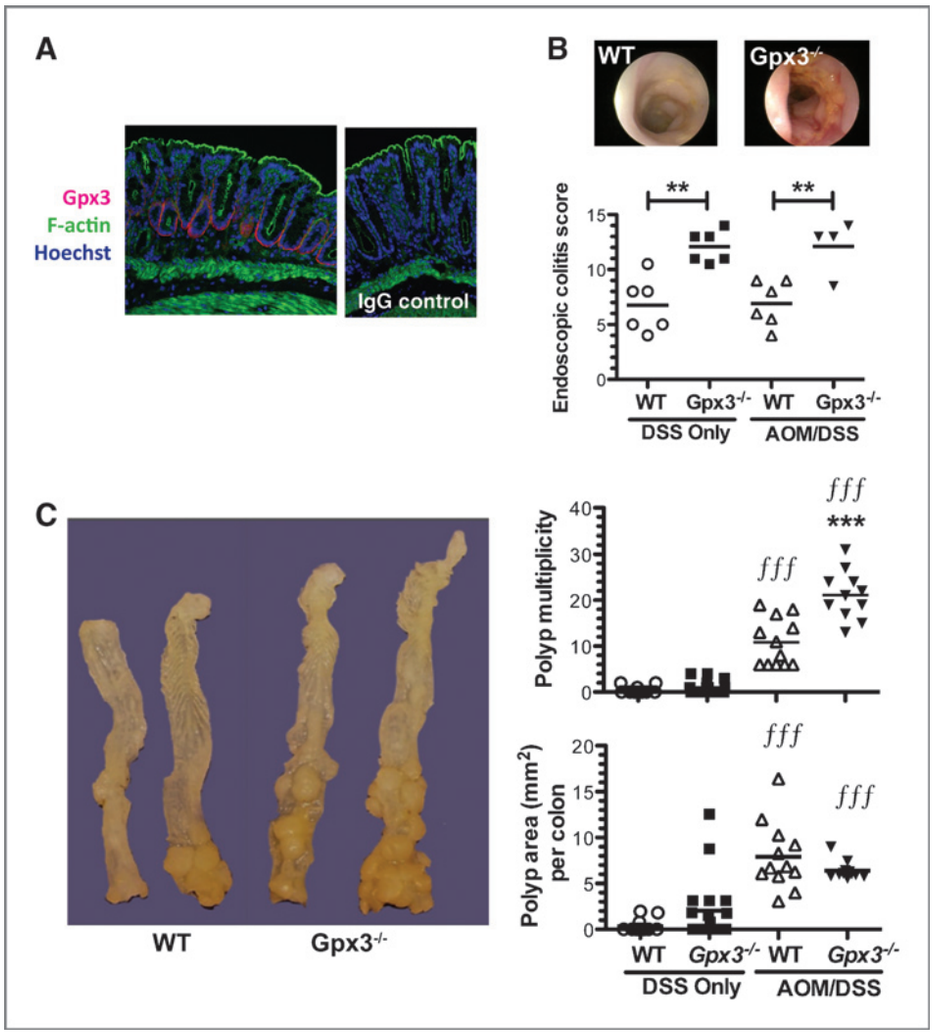

Figure 2. Gpx3 functions as a tumor suppressor in inflammatory carcinogenesis. A, immunofluorescence staining of normal WT colon. Gpx3 (red), F-actin (phalloidin, green), and Hoescht (blue) staining is shown (left). Immunoglobulin G (IgG) control is shown on the right (×60 magnification). B, representative colonoscopic images from WT (top left) or *Gpx3*$^{-/-}$ (top right) mice after 3 cycles of DSS and murine endoscopic colitis scoring using the murine endoscopic index of colitis severity. **, $P < 0.01$. C, representative gross specimens from the indicated genotype (left). Tumor multiplicity (top right) and polyp burden (bottom right) are shown; results were determined via calculation of the combined surface area ($\Sigma_{itot}\, SA_i = L_i \times W_i$) of all lesions in each colon. DSS only WT, $N = 13$; *Gpx3*$^{-/-}$, $N = 18$, AOM/DSS WT, $N = 12$; *Gpx3*$^{-/-}$, $N = 11$. ***, $P < 0.001$ between WT and *Gpx3*$^{-/-}$. ^{fff}, $P < 0.001$ DSS only versus AOM/DSS groups.

Altered intratumoral proliferation in the absence of Gpx3

Tumor number may be modified by increased cellular proliferation and/or survival or decreased apoptosis of transformed cells. Intratumoral proliferation rates were analyzed using *in situ* Ki67 staining. *Gpx3*$^{-/-}$ mice showed an average of 163.9 ± 14.1 Ki67^{+} cells per tumor HPF. WT mice, on the other hand, displayed 73.9 ± 15.1 Ki67^{+} cells per tumor HPF ($P = 0.0003$; Fig. 4A and B) indicating a significant increase in proliferation in *Gpx3*$^{-/-}$ tumors. No differences were seen in apoptotic indices as determined by terminal deoxynucleotidyl transferase–mediated dUTP nick end labeling (TUNEL) staining (Supplementary Fig. S5).

Increased nuclear and total β-catenin in *Gpx3*$^{-/-}$ tumors

Selenium deficiency in mice is predicted to stimulate the Wnt pathway (37). As the Wnt pathway is known to drive proproliferative and survival processes and is often hyperactive in the AOM/DSS model (38), we hypothesized that Wnt signaling, as evidenced by altered β-catenin localization, might be further perturbed in the absence of Gpx3. Therefore, we stained *Gpx3*$^{-/-}$ tumors for β-catenin localization. *Gpx3*$^{-/-}$ tumors showed a significant increase in both nuclear and total β-catenin, suggesting that the Wnt pathway is upregulated in these mice, even above that typically seen in AOM/DSS tumors (Fig. 4C and D; $P = 0.03$).

Increased M2 macrophage infiltrate and DNA damage in Gpx3$^{-/-}$ tumors

Macrophages are major modifiers of inflammation and resolution in response to injury. Their activity and motility is also significantly modified by selenium and selenoprotein modulation (39). Because *Gpx3*$^{-/-}$ mice show increased injury and inflammation in response to AOM and DSS (Fig. 3B and C), Gpx3 loss may influence intratumoral macrophage composition. *Gpx3*$^{-/-}$ tumors showed increased F4/80^{+} and Arg1^{+} protumorigenic M2 macrophages (17.1 ± 1.7 vs. 9.7 ± 1.5 F4/80^{+}/Arg1^{+} cells per tumor HPF; $P = 0.005$; Fig. 5A and B, bottom) and decreased F4/80^{+} and IL-1β^{+} antitumorigenic M1 macrophages (10.1 ± 1.7 vs. 18.6 ± 1.8 F4/80^{+}/IL-1β^{+} cells per tumor HPF; $P = 0.003$; Fig. 5A and B, top) compared with WT mice, suggesting that Gpx3 may have an impact on

Downloaded from http://aacrjournals.org/cancerres/article-pdf/73/3/1245/2692160/1245.pdf by guest on 24 May 2025

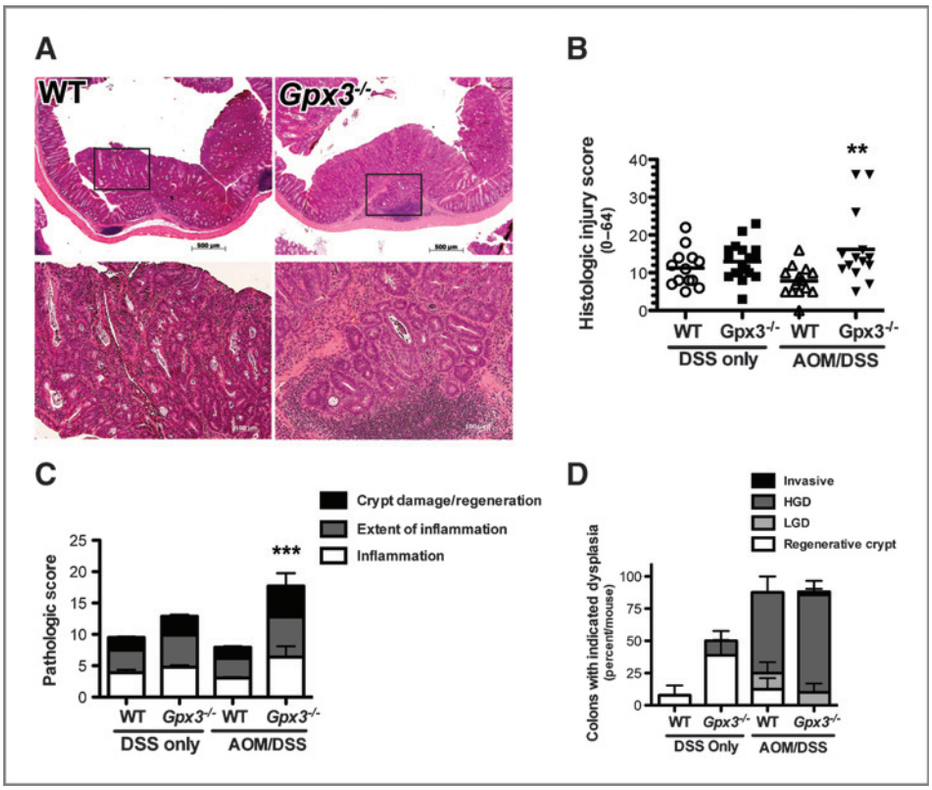

Figure 3. Increased histologic injury in *Gpx3*$^{-/-}$ colons. A, representative H&E staining from WT (×10 top, ×20 bottom left) or *Gpx3*$^{-/-}$ (×10 top, ×20 bottom right) colons. There is evidence for invasive adenocarcinoma in the *Gpx3*$^{-/-}$ tumor. B, histologic injury score for DSS only or AOM/DSS tissues. **, $P < 0.01$. C, division of the histologic injury scores from B into pathologic inflammation, extent, and crypt damage/regeneration scores for DSS only or AOM/DSS tissues. ***, $P < 0.001$. D, dysplasia grading (conducted by M.K. Washington) in WT and *Gpx3*$^{-/-}$ tumors expressed as invasive, high-grade dysplasia (HGD), low-grade dysplasia (LGD), or regenerative crypt. Results represent percentage of total tumors for each group within each grade.

macrophage polarization, promoting a skewing toward protumorigenic macrophage distribution.

ROS is produced during the AOM/DSS protocol as evidenced by increased expression of oxidative stress response genes (Fig. 1C and ref. 40). Because ROS can directly induce DNA damage via oxidation and deamination of DNA bases (41), and because DNA damage is an indicator of tumorigenesis risk, we wanted to determine whether loss of Gpx3

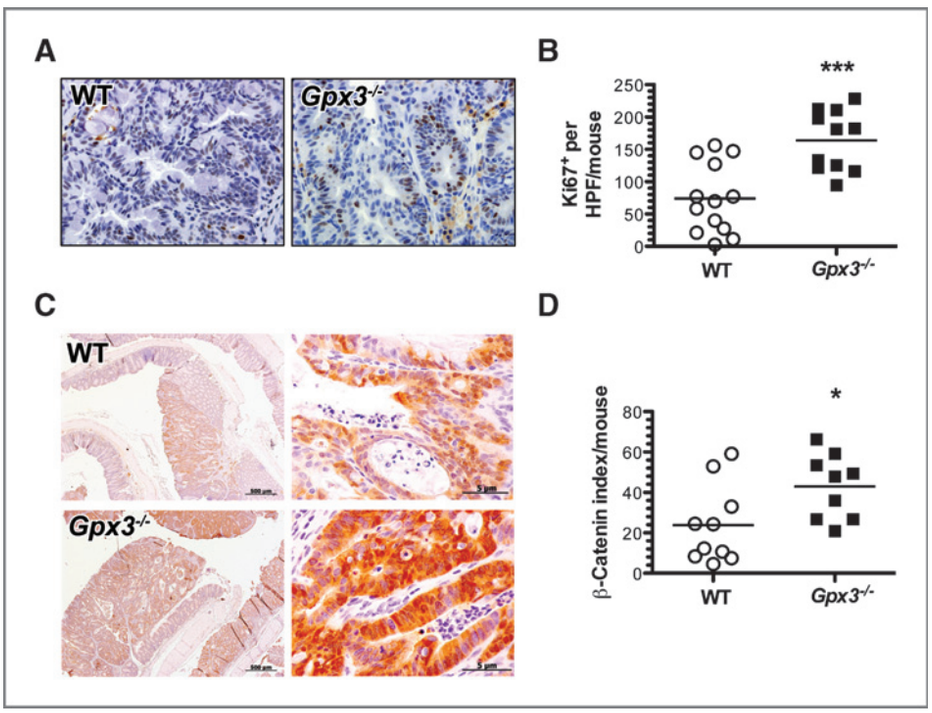

Figure 4. Increased intratumoral proliferation and nuclear β-catenin in *Gpx3*$^{-/-}$ tumors. α-Ki67 immunohistochemistry was conducted to identify actively proliferating cells. A, representative images of Ki67 staining in WT or *Gpx3*$^{-/-}$ tumors (×40 magnification). B, intratumoral proliferation index calculated from number of Ki67-positive cells per HPF in 20 HPF per mouse. ***, $P = 0.0003$. C, β-catenin expression and localization was determined via immunohistochemistry with β-catenin as per Materials and Methods (*Gpx3*$^{-/-}$, $N = 10$, WT, $N = 10$ tumors). Representative staining for β-catenin from WT or *Gpx3*$^{-/-}$ tumors (left, ×10 magnification; right, ×40 magnification). D, intratumoral β-catenin index calculated as described in Materials and Methods. *, $P = 0.03$.

Downloaded from http://aacrjournals.org/cancerres/article-pdf/73/3/1245/2692160/1245.pdf by guest on 24 May 2025

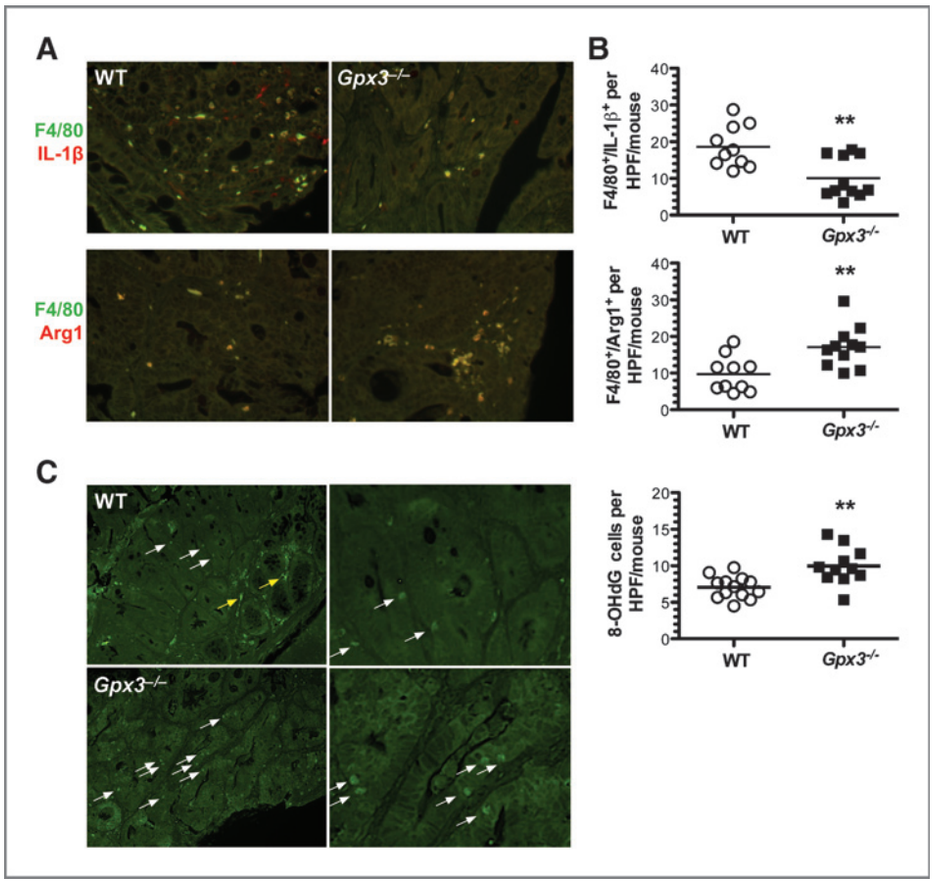

Figure 5. Increased M2 macrophages and evidence for oxidative DNA damage in *Gpx3*$^{-/-}$ tumors. Immunofluorescence for M1 (IL-1β^{+}, F4/80^{+}) and M2 (Arg1^{+}, F4/80^{+}) macrophage markers and 8-OHdG was conducted according to Materials and Methods. A, example images from WT top row or *Gpx3*$^{-/-}$ tumors. B, quantification of M1 (top) or M2 (bottom) macrophages per tumor HPF. **, $P < 0.01$. C, example images from WT (top row) or *Gpx3*$^{-/-}$ (bottom row) tumors. White arrow indicates positive staining in epithelial cells, yellow arrow indicates nonspecific staining. D, 8-OHdG quantification. **, $P < 0.01$. All images taken at ×40 magnification.

would lead to increased DNA damage. 8-Hydroxguanine (8-OHdG) staining was conducted to determine intratumoral DNA damage. In fact, *Gpx3*$^{-/-}$ tumors showed evidence for increased DNA damage compared with WT tumors (10.0 ± 0.8 vs. 7.1 ± 0.4 8-OHdG^{+} cells per HPF; $P = 0.002$; Fig. 5C).

GPX3 knockdown *in vitro* leads to increased ROS levels and DNA damage

To determine whether knockdown of *GPX3 in vitro* would recapitulate results seen *in vivo* we used shRNA to *GPX3* in the human colon cancer cell line Caco2. Caco2 cells were used as a model cell line because they express relatively higher levels of endogenous *GPX3* compared with other colon cancer cell lines (Supplementary Fig. S6A and S6B). shRNA-mediated knockdown resulted in decreased *GPX3* expression both at the mRNA and protein levels (Fig. 6A). At baseline, knockdown of *GPX3* had no impact on ROS production or DNA damage, though stimulation with H_2O_2 resulted in a significant increase in ROS (16; 1% vs. 7.3%; $P = 0.0019$), which was abolished with pretreatment with the H_2O_2 scavenger PEG-CAT. Furthermore, GPX3 knockdown had no effect on the activity of the oxidation-insensitive DCFH2^{+} analog, DCF^{+} (Fig. 6B, right graph, compare white with black bars), indicating the results obtained with DCFH2^{+} were due to changes in H_2O_2 concentrations as opposed to changes in uptake, ester cleavage, or efflux of the probe. There was also a concomitant increase in DNA damage (1,401 vs. 766 8-oxoguanosine mean fluorescence units; $P < 0.05$; Fig. 6C) in *GPX3* knockdown cells, consistent with data seen in tumors of *Gpx3*$^{-/-}$ mice. Thus, GPX3 does not seem to impact baseline oxidant parameters *in vitro* without application of a stressor, suggesting that its primary role is to buffer excessive H_2O_2 concentrations.

Knockdown of GPX3 *in vitro* leads to increased apoptosis and decreased contact-independent growth

Because our data suggest that Gpx3 functions as a tumor suppressor in colitis-associated carcinoma *in vivo*, we wanted to determine whether it modified cellular growth properties *in vitro* in the acute setting in an established colon cancer cell line. In contrast to *in vivo* modeling, in which there was no effect of *Gpx3* deletion on apoptosis, knockdown of *GPX3* in Caco2 cells led to increased apoptosis (26.8% vs. 15.6%; $P < 0.001$; Fig. 6D) and no difference in proliferation when exposed to the stressor H_2O_2. Also of note, knockdown of GPX3 led to decreased contact-independent growth in Matrigel colony formation assays (7.3 vs. 16.1 colonies; $P < 0.001$; Fig. 6E), indicating the potential for a dual role for Gpx3 as a tumor suppressor in chronic inflammatory carcinogenesis, whereas its loss in already established tumor cells (such as Caco2 cells) is detrimental to them.

Downloaded from http://aacrjournals.org/cancerres/article-pdf/73/3/1245/2692160/1245.pdf by guest on 24 May 2025

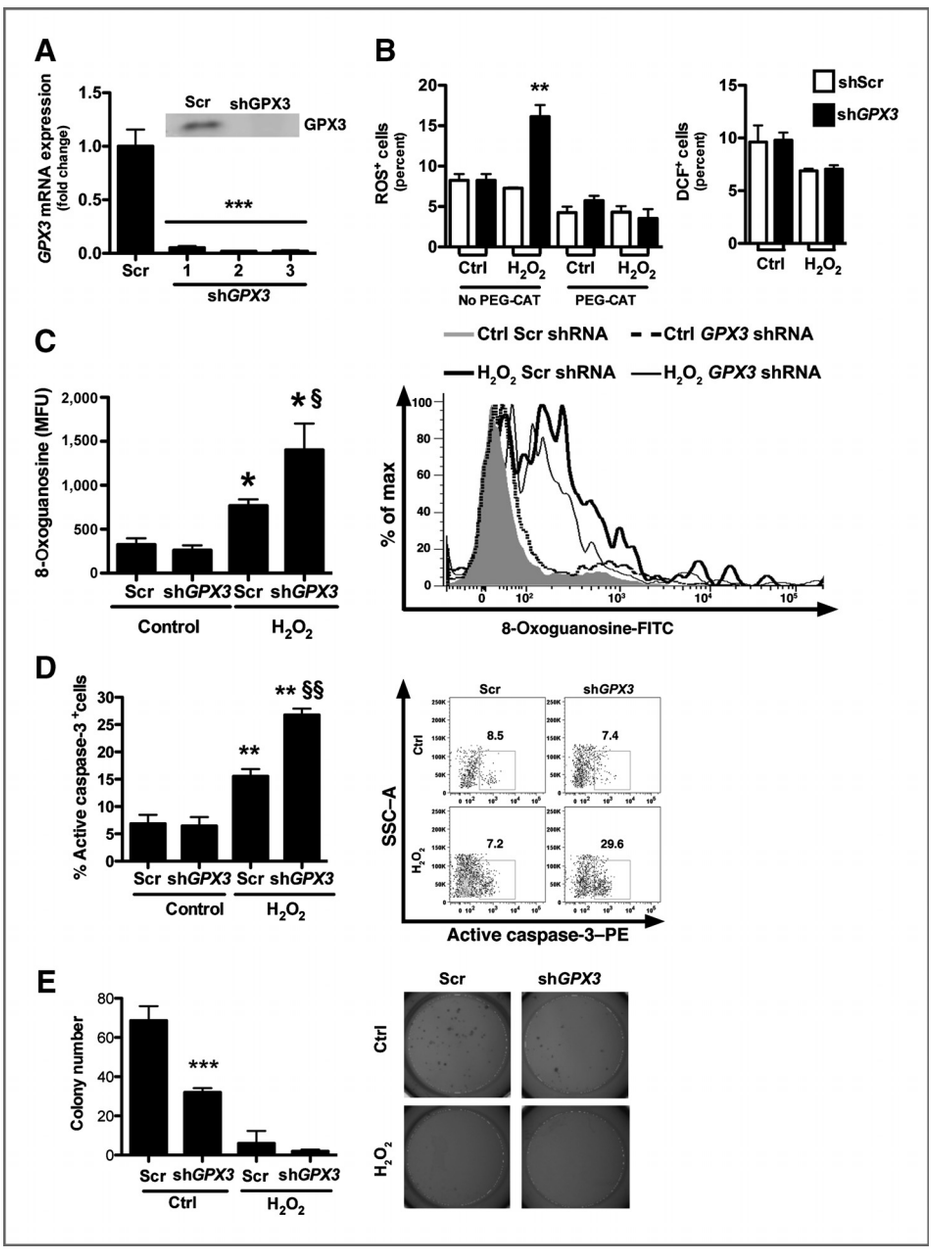

Figure 6. Increased ROS, DNA damage, and apoptosis and decreased soft agar colony formation post-GPX3 knockdown. A, GPX3 mRNA and protein (inset) expression after knockdown with GPX3-specific shRNA constructs in Caco2 cells. **, $P < 0.01$. B, quantification of percentage of ROS-positive cells ($DCFH2^+$) post-GPX3 knockdown in untreated or 200 μmol/L H_2O_2-treated Caco2 cells after pretreatment with the H_2O_2 scavenger PEG-CAT (left). **, $P < 0.01$. Quantification of percentage of DCF^+ (oxidation-insensitive analog) cells post-Gpx3 knockdown in untreated or H_2O_2-treated Caco2 cells (right). C, DNA damage as measured by 8-oxoguanosine–FITC flow cytometry in cells treated with scrambled or Gpx3-specific shRNAs and with or without H_2O_2 treatment. *, $P < 0.05$; ^{f}, $P < 0.05$. D, apoptosis, assessed as staining for active caspase-3 by flow cytometry (side-scatter-A; SSC-A). The percentage positive cells are shown. **, $P < 0.01$; ^{ff}, $P < 0.01$. E, colony formation assay in Matrigel in Gpx3 knockdown and scrambled control Caco2 cells with and without H_2O_2 treatment. ***, $P < 0.001$ Scr versus sh*GPX3* control.

Discussion

Chronic inflammation, as seen in ulcerative colitis and Crohn's colitis, predisposes to malignancy (2). In fact, the risk for cancer is increased 6-fold in patients with IBD compared with the general population (4). Although the relationship between chronic inflammation and carcinogenesis is complicated and imprecisely understood, it is hypothesized that the excess ROS and reactive nitrogen species (RNS) accompanying inflammation contribute to malignancy. During chronic inflammation superoxide is produced at rates that overwhelm antioxidant systems (42, 43). When reactive oxygen and nitrogen species are not cleared efficiently, they begin to react with lipids, proteins, and DNA (44). More specifically, oxidative DNA damage leads to C/G base pair mutations, which lead to an increased frequency of C:G→T:A transversion (45), a mutation that is most frequently observed in mutated proto-oncogenes and tumor suppressor genes (46). GPX3 is an extracellular glutathione peroxidase that is able to abrogate ROS and is postulated to protect from carcinogenesis via these activities, although this has up to now not been rigorously tested using reverse genetics. We applied this approach to define the role of Gpx3 in inflammatory carcinogenesis and now show that Gpx3 is indeed a potent inhibitor of tumor promotion and progression. The impact of Gpx3 loss on tumorigenesis is likely mediated by increased inflammation and DNA damage as well as increased intratumoral proliferation that probably results

Downloaded from http://aacrjournals.org/cancerres/article-pdf/73/3/1245/2692160/1245.pdf by guest on 24 May 2025

from an increase in β-catenin nuclear translocation and Wnt stimulation. Loss of Gpx3 in the AOM/DSS colitis-associated carcinoma model leads to increased tumor number but not size. *Gpx3*$^{-/-}$ tumors also showed increased tumor staging suggesting that its loss also contributes to progression. In fact, one *Gpx3*$^{-/-}$ tumor showed local invasion, a characteristic that is not normally seen as the result of the AOM/DSS protocol. This is significant because it supports epidemiologic data that show that throughout the course of colorectal cancer progression, GPX3 expression is decreased (18).

While the *in vivo* reverse genetic experiments using the *Gpx3*$^{-/-}$ mice in the AOM/DSS protocol model allowed us to decipher the cumulative affects of the absence of *Gpx3* throughout the full spectrum of transformation from normal cells to tumor cells, *in vitro* experiments were conducted in established cancer cells (Caco2) to isolate the contribution of GPX3 to maintenance or promotion. As noted *in vivo*, GPX3 loss resulted in increased DNA damage. Of interest, knockdown of GPX3 in Caco2 cells resulted in a decrease in contact-independent growth and increase in apoptosis in response to H_2O_2, indicating that the acute absence of Gpx3 is detrimental to established carcinoma growth.

Our data show that there is increased inflammation and crypt damage and regeneration in *Gpx3*$^{-/-}$ AOM/DSS mice as compared with WT mice. Furthermore, this inflammation occurred despite a decrease in M1 and increase in M2 macrophages. It is theorized that M1 macrophages, which normally serve as proinflammatory cells, are tumoricidal and downregulated during cancer development, whereas M2 macrophages, which normally aid in the resolution of the inflammatory response, are protumorigenic and upregulated within the tumor microenvironment (47). Thus Gpx3 loss likely contributes to differential macrophage activation or recruitment that further supports tumor growth and survival. This is an interesting finding as selenoprotein deficiency leads to diminished macrophage migration (39) and selenium enhances the capacity of a host to generate cytotoxic lymphocytes and macrophages to destroy tumor cells (48, 49). Thus, our data suggest that at least part of the immune cell modifying properties of selenium are actuated by Gpx3.

Thus far, our data support a tumor suppressor role for Gpx3 via clearance of ROS. Upon knockdown of Gpx3 in the human colorectal cancer cell line Caco2, we saw an induction of ROS as well as an increase in DNA damage resulting from H_2O_2 treatment that supports our *in vivo* data. Contrary to what was originally expected, knockdown of Gpx3 did not alter proliferation at baseline or during stress as was seen *in vivo*. Instead, apoptosis was increased in response to H_2O_2 administration, a result that would be expected in cells that do not harbor the capacity to deal with oxidative stress due to the loss of the antioxidant Gpx3. Even at baseline, knockdown of Gpx3 in Caco2 cells resulted in a decrease in contact-independent cell growth, a marker of tumorigenicity. This is contrary to our *in vivo* findings in which Gpx3 served as a tumor suppressor. Although initially surprising, we hypothesize that the tumor suppressive role of Gpx3 exists in its ability to prevent the initiation and malignant transformation *in vivo*, but in cells that are already malignant, Gpx3 is able to promote tumorigenesis by protecting them from apoptosis. This also likely explains why, despite having higher proliferation rates, the tumors of *Gpx3*$^{-/-}$ mice are not larger than those of WT mice. It may be that, upon the application of a stressor such as DSS, malignant cells in *Gpx3*$^{-/-}$ mice are dying more rapidly than those in WT mice and stabilizing the tumor size.

In conclusion, we show that removal of Gpx3 enhances inflammation and injury, proliferation, nuclear β-catenin, and DNA damage in tumors of mice subjected to an inflammatory carcinogenesis protocol. The net effect of these changes leads to an increase in tumor promotion in response to Gpx3 loss. Thus, Gpx3 seems to serve as a tumor suppressor in colitis-associated carcinoma. These studies provide insight into disease pathogenesis and indicate that at least one of the selenoproteins that modifies carcinogenesis is Gpx3 and that it may serve as a substrate for translational investigations in colitis-associated carcinoma.

Disclosure of Potential Conflicts of Interest

No potential conflicts of interest were disclosed.

Authors' Contributions

Conception and design: C.W. Barrett, W. Ning, K.E. Hill, R. Chaturvedi, K.T. Wilson, R.F. Burk, C.S. Williams
Development of methodology: C.W. Barrett, W. Ning, K.E. Hill, R. Chaturvedi, R.F. Burk, C.S. Williams
Acquisition of data (provided animals, acquired and managed patients, provided facilities, etc.): C.W. Barrett, W. Ning, J.J. Smith, M.K. Washington, K. E. Hill, R. Chaturvedi, C.S. Williams
Analysis and interpretation of data (e.g., statistical analysis, biostatistics, computational analysis): C.W. Barrett, W. Ning, X. Chen, J.J. Smith, M.K. Washington, K.E. Hill, K.T. Wilson, C.S. Williams
Writing, review, and/or revision of the manuscript: C.W. Barrett, W. Ning, M.K. Washington, K.E. Hill, L.A. Coburn, R.M. Peek, K.T. Wilson, R.F. Burk, C.S. Williams
Administrative, technical, or material support (i.e., reporting or organizing data, constructing databases): W. Ning, J.J. Smith, C.S. Williams
Study supervision: W. Ning, C.S. Williams

Acknowledgments

The authors thank Teri Stevenson for help with animal husbandry, members of the Williams and Burk laboratories for thoughtful discussions about this research project. The authors also thank Virginia Winfrey for her help with immunofluorescent staining and imaging.

Grant Support

This work was supported by the NIH grants DK080221 (C.S. Williams), R01 DK82813 (R.F. Burk), P50CA095103 (M.K. Washington), AT004821 (K.T. Wilson), AT004821-S1 (K.T. Wilson), DK053620 (K.T. Wilson), and 1F31CA167920 (C.W. Barrett), Merit Review Grants from the Office of Medical Research, Department of Veterans Affairs 1I01BX001426 (C.S. Williams) and 1I01BX001453-01 (K.T. Wilson), and ACS-RSG 116552 (C.S. Williams). Core Services performed through Vanderbilt University Medical Center's Digestive Disease Research Center supported by NIH grant P30DK058404 (R.M. Peek) and the Vanderbilt Ingram Cancer Center shared resources P30CA068485.

The costs of publication of this article were defrayed in part by the payment of page charges. This article must therefore be hereby marked *advertisement* in accordance with 18 U.S.C. Section 1734 solely to indicate this fact.

Received August 10, 2012; revised November 28, 2012; accepted November 29, 2012; published OnlineFirst December 5, 2012.

Downloaded from http://aacrjournals.org/cancerres/article-pdf/73/3/1245/2692160/1245.pdf by guest on 24 May 2025

References

1. Dincer Y, Erzin Y, Himmetoglu S, Gunes KN, Bal K, Akcay T. Oxidative DNA damage and antioxidant activity in patients with inflammatory bowel disease. Dig Dis Sci 2007;52:1636–41.
2. Itzkowitz SH, Yio X. Inflammation and cancer IV. Colorectal cancer in inflammatory bowel disease: the role of inflammation. Am J Physiol Gastrointest Liver Physiol 2004;287:G7–17.
3. Rachmilewitz D, Stamler JS, Bachwich D, Karmeli F, Ackerman Z, Podolsky DK. Enhanced colonic nitric oxide generation and nitric oxide synthase activity in ulcerative colitis and Crohn's disease. Gut 1995;36:718–23.
4. Ekbom A, Helmick C, Zack M, Adami HO. Ulcerative colitis and colorectal cancer. A population-based study. N Engl J Med 1990;323: 1228–33.
5. Irons R, Carlson BA, Hatfield DL, Davis CD. Both selenoproteins and low molecular weight selenocompounds reduce colon cancer risk in mice with genetically impaired selenoprotein expression. J Nutr 2006;136:1311–7.
6. Hudson TS, Carlson BA, Hoeneroff MJ, Young HA, Sordillo L, Muller WJ, et al. Selenoproteins reduce susceptibility to DMBA-induced mammary carcinogenesis. Carcinogenesis 2012;33:1225–30.
7. Maiorino M, Aumann KD, Brigelius-Flohe R, Doria D, van den Heuvel J, McCarthy J, et al. Probing the presumed catalytic triad of selenium-containing peroxidases by mutational analysis of phospholipid hydroperoxide glutathione peroxidase (PHGPx). Biol Chem Hoppe Seyler 1995;376:651–60.
8. Brigelius-Flohe R. Tissue-specific functions of individual glutathione peroxidases. Free Radic Biol Med 1999;27:951–65.
9. Olson GE, Whitin JC, Hill KE, Winfrey VP, Motley AK, Austin LM, et al. Extracellular glutathione peroxidase (Gpx3) binds specifically to basement membranes of mouse renal cortex tubule cells. Am J Physiol Renal Physiol 2010;298:F1244–53.
10. Maeda K, Okubo K, Shimomura I, Mizuno K, Matsuzawa Y, Matsubara K. Analysis of an expression profile of genes in the human adipose tissue. Gene 1997;190:227–35.
11. Chu FF, Esworthy RS, Doroshow JH, Doan K, Liu XF. Expression of plasma glutathione peroxidase in human liver in addition to kidney, heart, lung, and breast in humans and rodents. Blood 1992;79: 3233–8.
12. Tham DM, Whitin JC, Kim KK, Zhu SX, Cohen HJ. Expression of extracellular glutathione peroxidase in human and mouse gastrointestinal tract. Am J Physiol 1998;275(6 Pt 1):G1463–71.
13. Avissar N, Ornt DB, Yagil Y, Horowitz S, Watkins RH, Kerl EA, et al. Human kidney proximal tubules are the main source of plasma glutathione peroxidase. Am J Physiol 1994;266(2 Pt 1):C367–75.
14. Burk RF, Olson GE, Winfrey VP, Hill KE, Yin D. Glutathione peroxidase-3 produced by the kidney binds to a population of basement membranes in the gastrointestinal tract and in other tissues. Am J Physiol Gastrointest Liver Physiol 2011;301:G32–8.
15. Chen B, Rao X, House MG, Nephew KP, Cullen KJ, Guo Z. GPx3 promoter hypermethylation is a frequent event in human cancer and is associated with tumorigenesis and chemotherapy response. Cancer Lett 2011;309:37–45.
16. Zhang X, Yang JJ, Kim YS, Kim KY, Ahn WS, Yang S. An 8-gene signature, including methylated and down-regulated glutathione peroxidase 3, of gastric cancer. Int J Oncol 2010;36:405–14.
17. Yu YP, Yu G, Tseng G, Cieply K, Nelson J, Defrances M, et al. Glutathione peroxidase 3, deleted or methylated in prostate cancer, suppresses prostate cancer growth and metastasis. Cancer Res 2007;67:8043–50.
18. Murawaki Y, Tsuchiya H, Kanbe T, Harada K, Yashima K, Nozaka K, et al. Aberrant expression of selenoproteins in the progression of colorectal cancer. Cancer Lett 2008;259:218–30.
19. Esworthy RS, Aranda R, Martin MG, Doroshow JH, Binder SW, Chu FF. Mice with combined disruption of Gpx1 and Gpx2 genes have colitis. Am J Physiol Gastrointest Liver Physiol 2001;281:G848–55.
20. Chu FF, Esworthy RS, Doroshow JH. Role of Se-dependent glutathione peroxidases in gastrointestinal inflammation and cancer. Free Radic Biol Med 2004;36:1481–95.
21. Krehl S, Loewinger M, Florian S, Kipp AP, Banning A, Wessjohann LA, et al. Glutathione peroxidase-2 and selenium decreased inflammation and tumors in a mouse model of inflammation-associated carcinogenesis whereas sulforaphane effects differed with selenium supply. Carcinogenesis 2012;33:620–8.
22. D'Odorico A, D'Inca R, Mestriner C, Di Leo V, Ferronato A, Sturniolo GC. Influence of disease site and activity on peripheral neutrophil function in inflammatory bowel disease. Dig Dis Sci 2000;45:1594–600.
23. Eaden J. Review article: colorectal carcinoma and inflammatory bowel disease. Aliment Pharmacol Ther 2004;20(Suppl 4):24–30.
24. Mayer R, Wong WD, Rothenberger DA, Goldberg SM, Madoff RD. Colorectal cancer in inflammatory bowel disease: a continuing problem. Dis Colon Rectum 1999;42:343–7.
25. Greten FR, Eckmann L, Greten TF, Park JM, Li ZW, Egan LJ, et al. IKKbeta links inflammation and tumorigenesis in a mouse model of colitis-associated cancer. Cell 2004;118:285–96.
26. Fukata M, Chen A, Vamadevan AS, Cohen J, Breglio K, Krishnareddy S, et al. Toll-like receptor-4 promotes the development of colitis-associated colorectal tumors. Gastroenterology 2007;133:1869–81.
27. Popivanova BK, Kitamura K, Wu Y, Kondo T, Kagaya T, Kaneko S, et al. Blocking TNF-alpha in mice reduces colorectal carcinogenesis associated with chronic colitis. J Clin Invest 2008;118:560–70.
28. Barrett CW, Fingleton B, Williams A, Ning W, Fischer MA, Washington MK, et al. MTGR1 is required for tumorigenesis in the murine AOM/DSS colitis-associated carcinoma model. Cancer Res 2011; 71:1302–12.
29. Grivennikov S, Karin E, Terzic J, Mucida D, Yu GY, Vallabhapurapu S, et al. IL-6 and Stat3 are required for survival of intestinal epithelial cells and development of colitis-associated cancer. Cancer Cell 2009;15: 103–13.
30. Uronis JM, Muhlbauer M, Herfarth HH, Rubinas TC, Jones GS, Jobin C. Modulation of the intestinal microbiota alters colitis-associated colorectal cancer susceptibility. PLoS ONE 2009;4:e6026.
31. Dieleman LA, Palmen MJ, Akol H, Bloemena E, Pena AS, Meuwissen SG, et al. Chronic experimental colitis induced by dextran sulphate sodium (DSS) is characterized by Th1 and Th2 cytokines. Clin Exp Immunol 1998;114:385–91.
32. Becker C, Fantini MC, Neurath MF. High resolution colonoscopy in live mice. Nat Protoc 2006;1:2900–4.
33. Lawrence RA, Burk RF. Glutathione peroxidase activity in selenium-deficient rat liver. Biochem Biophys Res Commun 1976;71:952–8.
34. Paglia DE, Valentine WN. Studies on the quantitative and qualitative characterization of erythrocyte glutathione peroxidase. J Lab Clin Med 1967;70:158–69.
35. Chaturvedi R, Asim M, Romero-Gallo J, Barry DP, Hoge S, de Sablet T, et al. Spermine oxidase mediates the gastric cancer risk associated with *Helicobacter pylori* CagA. Gastroenterology 2011;141:1696–708 e1–2.
36. Becker C, Fantini MC, Wirtz S, Nikolaev A, Kiesslich R, Lehr HA, et al. *In vivo* imaging of colitis and colon cancer development in mice using high resolution chromoendoscopy. Gut 2005;54:950–4.
37. Kipp A, Banning A, van Schothorst EM, Meplan C, Schomburg L, Evelo C, et al. Four selenoproteins, protein biosynthesis, and Wnt signalling are particularly sensitive to limited selenium intake in mouse colon. Mol Nutr Food Res 2009;53:1561–72.
38. Tanaka T, Kohno H, Suzuki R, Yamada Y, Sugie S, Mori H. A novel inflammation-related mouse colon carcinogenesis model induced by azoxymethane and dextran sodium sulfate. Cancer Sci 2003;94: 965–73.
39. Carlson BA, Yoo MH, Sano Y, Sengupta A, Kim JY, Irons R, et al. Selenoproteins regulate macrophage invasiveness and extracellular matrix-related gene expression. BMC Immunol 2009;10:57.
40. Yasui Y, Tanaka T. Protein expression analysis of inflammation-related colon carcinogenesis. J Carcinog 2009;8:10.
41. Bartsch H, Nair J. Potential role of lipid peroxidation derived DNA damage in human colon carcinogenesis: studies on exocyclic base adducts as stable oxidative stress markers. Cancer Detect Prev 2002;26:308–12.

Downloaded from http://aacrjournals.org/cancerres/article-pdf/73/3/1245/2692160/1245.pdf by guest on 24 May 2025

42. Fridovich I. Fundamental aspects of reactive oxygen species, or what's the matter with oxygen? Ann N Y Acad Sci 1999;893:13–8.
43. Muscoli C, Cuzzocrea S, Riley DP, Zweier JL, Thiemermann C, Wang ZQ, et al. On the selectivity of superoxide dismutase mimetics and its importance in pharmacological studies. Br J Pharmacol 2003;140: 445–60.
44. Dix TA, Hess KM, Medina MA, Sullivan RW, Tilly SL, Webb TL. Mechanism of site-selective DNA nicking by the hydrodioxyl (perhydroxyl) radical. Biochemistry 1996;35:4578–83.
45. Cheng KC, Cahill DS, Kasai H, Nishimura S, Loeb LA. 8-Hydroxyguanine, an abundant form of oxidative DNA damage, causes G—T and A—C substitutions. J Biol Chem 1992;267:166–72.
46. Hussain SP, Harris CC. Molecular epidemiology of human cancer: contribution of mutation spectra studies of tumor suppressor genes. Cancer Res 1998;58:4023–37.
47. Sica A, Bronte V. Altered macrophage differentiation and immune dysfunction in tumor development. J Clin Invest 2007;117:1155–66.
48. Kiremidjian-Schumacher L, Roy M, Wishe HI, Cohen MW, Stotzky G. Regulation of cellular immune responses by selenium. Biol Trace Elem Res 1992;33:23–35.
49. Kiremidjian-Schumacher L, Roy M, Wishe HI, Cohen MW, Stotzky G. Supplementation with selenium and human immune cell functions. II. Effect on cytotoxic lymphocytes and natural killer cells. Biol Trace Elem Res 1994;41:115–27.

Downloaded from http://aacrjournals.org/cancerres/article-pdf/73/3/1245/2692160/1245.pdf by guest on 24 May 2025